CARBON 59 (2013) 167–175

Available at www.sciencedirect.com

SciVerse ScienceDirect

journal homepage: www.elsevier.com/locate/carbon

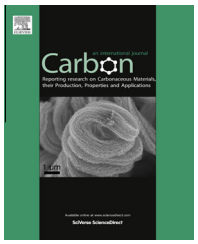

Reduced wear and friction enabled by graphene layers on sliding steel surfaces in dry nitrogen ☆

Diana Berman [a], *Ali Erdemir* [b], *Anirudha V. Sumant* [a,*]

[a] *Center for Nanoscale Materials, Argonne National Laboratory, 9700 S. Cass Ave., Argonne, IL 60439, USA*
[b] *Energy Systems Division, Argonne National Laboratory, 9700 S. Cass Ave., Argonne, IL 60439, USA*

ARTICLE INFO

Article history:
Received 10 January 2013
Accepted 5 March 2013
Available online 13 March 2013

ABSTRACT

We report on the friction and wear behavior of graphene-lubricated 440C steel test pairs in dry nitrogen under different loads. Tribological test results have revealed that a few-layer graphene is able to drastically reduce the wear and the coefficient of friction (COF) of 440C steel during the initial sliding regime and under low load conditions. Specifically, the COF has been reduced from ≈1 for bare steel to 0.15 for steel covered by a low concentration of graphene flakes. Such low COFs have persisted for thousands of sliding passes, even though the graphene layers formed on sliding surfaces have not been continuous or continuously replenished; they were made of a few sheets of graphene. The wear rates of the steel test pairs have been also reduced (by as much as two orders of magnitude), again despite the very sporadic and thin nature of the graphene layers. A possible explanation for the low friction and wear reduction is that graphene as a two-dimensional material shears easily at the sliding contact interface and, hence, provides low friction.

1. Introduction

Reducing energy and material losses in moving mechanical systems due to friction and wear still remains one of the greatest challenges of our time [1,2]. Worldwide concerted efforts continue in developing new materials, coatings, and lubricants that can potentially provide low friction and wear even under severe operating conditions. Many dedicated studies have identified numerous types of tribological mechanisms for different kinds of materials operating under different environments, temperatures, or lubricated test conditions [3,4]. Most traditional methods of controlling friction and wear involve the uses of solid and liquid lubricants at sliding contact interfaces [5–7]. However, finding the most effective lubricant that is also environmental friendly and cost-competitive [8] remains difficult. One of the emerging self-lubricating materials is graphene, which has been widely studied for its unusual thermal, electrical, mechanical, and recently, tribological properties [9–15]. However, previous studies on graphene tribology have mostly focused on nano- to microscale friction and wear behavior [16–20] and these studies have greatly increased our understanding of the fundamental lubrication mechanisms involved. However, macro/mesoscale tribological studies of graphene have remained relatively unexplored but urgently needed to realize graphene's full potential for diverse tribological applications. At present, using various forms of carbon-based nanomaterials (i.e., nanotube, nano-onions, nano-diamond, etc.) to reduce the

☆ The submitted manuscript has been created by UChicago Argonne, LLC, Operator of Argonne National Laboratory ("Argonne"). Argonne, a US Department of Energy Office of Science Laboratory, is operated under Contract No. DE-AC02-06CH11357. The US Government retains for itself, and others acting on its behalf, a paid-up nonexclusive, irrevocable worldwide license in said article to reproduce, prepare derivative works, distribute copies to the public, and perform publicly and display publicly, by or on behalf of the Government.

* *Corresponding author.*
E-mail address: sumant@anl.gov (A.V. Sumant).

0008-6223/$ - see front matter © 2013 Published by Elsevier Ltd.
http://dx.doi.org/10.1016/j.carbon.2013.03.006

wear in general is gaining high momentum [21–24]. Graphene is also being tried as an oil additive [25], and in the development of polymer-matrix composites [26] providing impressive lubrication and mechanical properties, thus resulting in excellent wear resistance under a wide range of test conditions [27]. Other solid lubricants such as MoS_2, Pb–Mo–S or graphite can also provide low friction and wear [1,28]. However, the majority of them require large amount and, often times, full coverage of lubricant material [29]. Also, specific deposition processes (such as high temperature processing [30] or magnetron sputtering [31,32]) limit the application of these lubricants. In contrast, in this study, we aim to demonstrate that using very little or few layers of graphene on sliding steel surfaces can lead to remarkable reductions in their friction and wear, thus further corroborating its potential to improve efficiency and durability of many moving mechanical systems. In a previous study, we reported dramatic reductions in friction and wear for steel tribo-pairs that were continuously lubricated with graphene layers under humid air conditions [33]. Also, graphene's great ability to inhibit tribo-corrosion under humid conditions was confirmed. In this study, we concentrated our attention on the friction and wear behavior of graphene layers (2–3 sheets) on steel plates in dry nitrogen as a function of load. It is well known that bulk graphite (a source of graphene) works the best in humid environments but fails to provide low friction and wear in inert, dry, or vacuum environments [34,35]. One of the major objectives of this study was to ascertain whether graphene behaves similarly to bulk graphite under dry and inert test conditions. In our study, graphene flakes were applied on sliding surfaces by spreading graphene-containing ethanol solution on the surface and then evaporating ethanol to leave the solution processed graphene flakes (SPGF) behind as a non-continuous film that is only a few layers thick.

2. Experimental procedure

Tribological studies were performed in dry nitrogen environment (900 mbar) at room temperature using a CSM high vacuum tribometer with a ball on disk contact geometry. The stainless steel flat samples (AISI 440C grade) were initially cleaned by sonication in acetone and then in isopropanol in an ultrasonic bath to remove any contamination that may have been left from the sample preparation steps. As a counterpart, the stainless steel ball (440C grade) of 9.5 mm diameter was used. Both the flat and ball samples had Vickers micro indentation hardness values of about 7 GPa and their rms roughness measured by the 3D profilometer was R_q = 15 nm. The normal load during the tribotests was varied from 1 N to 5 N with detailed study performed at 2 N load and a wear track of 15 mm radius was used in each flat. Sliding speed during the tests was 60 rpm (or 9.4 cm/s).

For the tests performed in dry nitrogen environment, the vacuum tribometer was initially pumped twice down to 10^{-5} mbar base pressure with nitrogen backflow while the oxygen sensor confirmed less than 0.01% of oxygen presence.

As the graphene source, we used commercially available ethanol solution processed graphene (SPG) from Graphene Supermarket Inc. The SPG solution was prepared by chemical exfoliation of the highly oriented pyrolytic graphite (HOPG) in ethanol. The weight concentration of graphene was 1 mg/L containing mostly single layer graphene. Small SPG amount (2–3 drops or 0.1–0.15 mL of solution per 1 cm^2) was applied on the highly polished surfaces of stainless steel plates in a colloidal liquid state and the liquid ethanol part was evaporated in dry nitrogen environment to reduce graphene oxidation. Formation of a graphene layer on the steel surface has been confirmed by an Invia Confocal Raman Microscope using the red laser light (λ = 633 nm). As shown in Fig. 1, after evaporation of ethanol, a grayish deposit was left on the steel surface and the presence of small 2–3 layers of graphene flakes in the deposit was confirmed by the characteristic Raman bands indicated via the Raman microscope used in our study (Fig. 1). The Raman spectra analysis of G and 2D peaks shows that we supplied few layers (2–3) of graphene [36]. The presence of defect peak D can be explained by partial oxidation of graphene during deposition process as well as non-planar deposition of the flakes. As it can be seen from the Fig. 1a, the size of the deposited graphene flakes varies, but does not extend 2 μm in diameter. Also, the coverage of the deposited flakes (by the area) does not exceed 25% of the total surface area.

The imaging of the wear scars and tracks was performed by an Olympus UC30 Microscope. The wear rates on the ball and the flat side were determined using a 3D Non-contact MicroXam profilometer.

3. Results and discussion

3.1. *Effect of SPGF on friction and wear during initial cycling*

To investigate the effect of graphene on tribological performance of 440C steel, a baseline test for 600 cycles was carried out with bare steel in dry nitrogen environment under a 2 N load (average Hertz contact pressure is 0.41 GPa). As it is shown in Fig. 2a, the frictional behavior of bare steel is rather unsteady and fluctuates substantially due to adhesive wear and perhaps third-body wear debris accumulation within the sliding contact interface. In the absence of oxygen and/or humidity, this stainless steel test pair performs very poorly and leads to significantly high friction and wear again, perhaps due to the severe adhesion and plowing. Together, these two phenomena may cause roughening of the wear track and scar which further increases friction especially during the later stages of sliding test as shown in Fig. 2a. After SPGF deposition on the steel plate side however, we noticed a dramatic change in frictional behavior. Specifically, when we repeat the same tests on graphene layers deposited on the 440C steel flat, we achieved friction coefficients of 0.15 to 0.3 and observe no evidence of major stick–slip type of sliding behavior (see Fig. 2a). Note that at the start of sliding test, the coefficient of friction of SPGF treated steel flat was about 0.15 and then went up as high as 0.3; but toward the end, it stabilized at around 0.18 (which is nearly 6 times lower than what was observed on the bare or uncoated 440C steel sample).

Another important aspect is the graphene's influence on wear behavior of the steel. For this purpose, we also investigated the wear performance of 440C balls and flats with and without SPGF deposition on sliding surfaces.

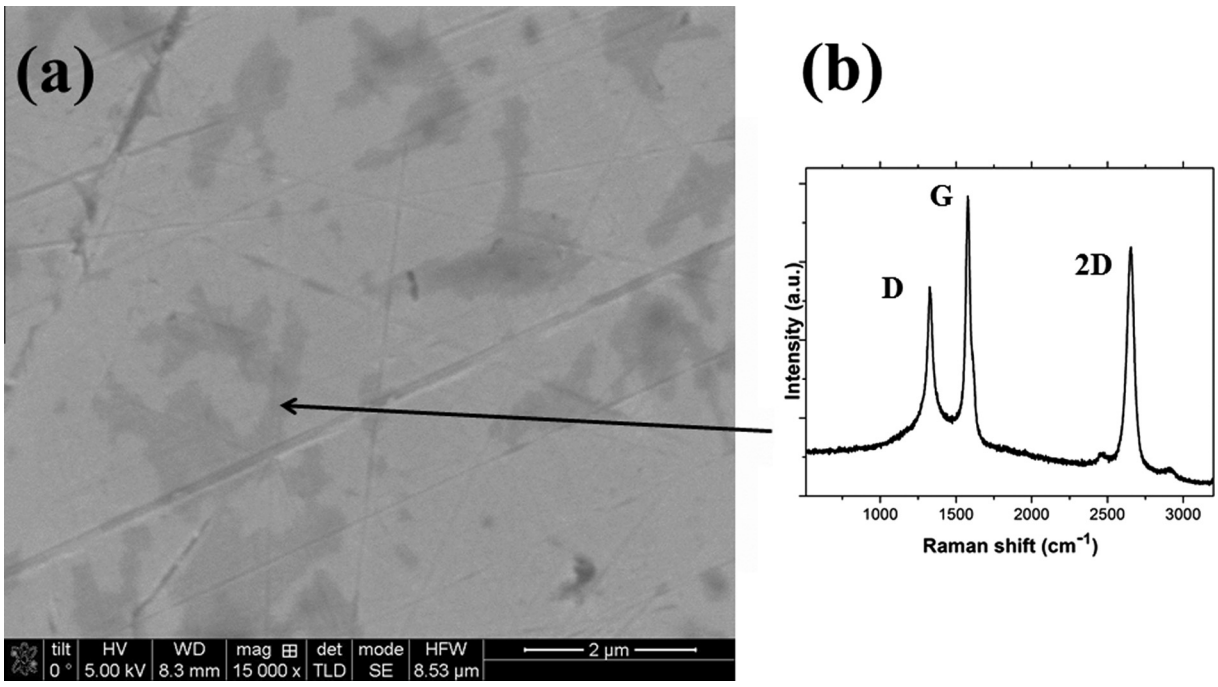

Fig. 1 – SEM image of as deposited graphene flakes (a) and Raman spectrum of one of the flakes on steel plate (b). D peak indicates presence of defects in the deposited graphene while the G and 2D peaks help to determine the number of deposited layers.

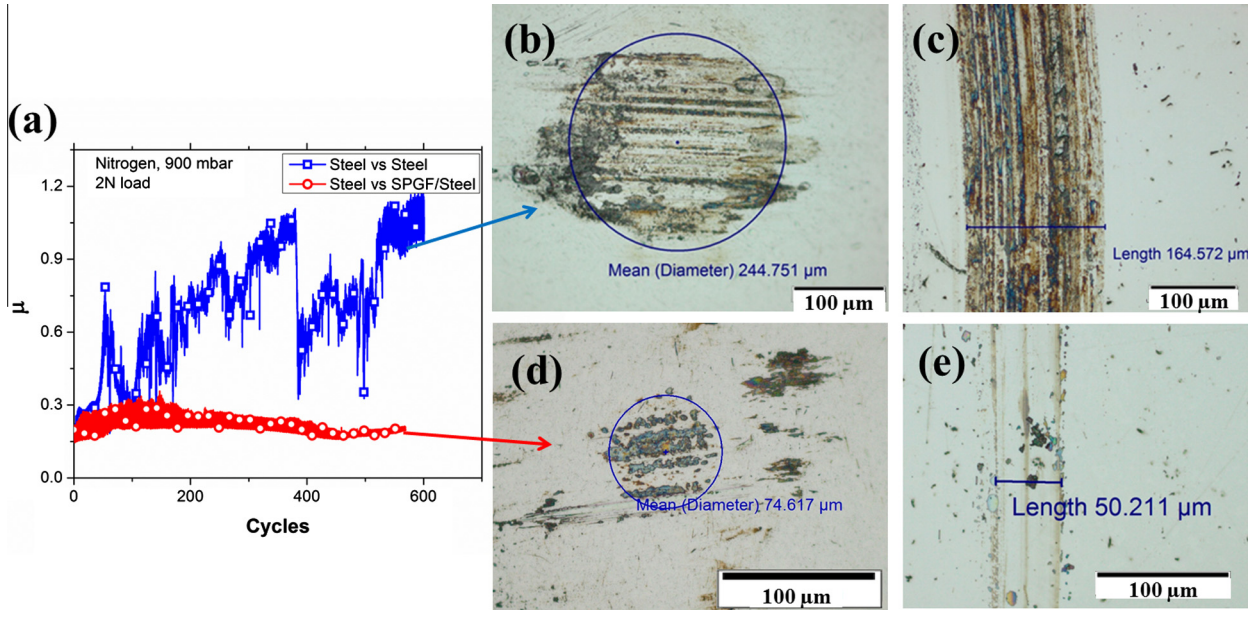

Fig. 2 – Coefficient of friction for steel with and without SPGF (a) and ball and plate wear after steel against steel (b and c) and against SPGF/steel (d and e) tests for 600 cycles.

Fig. 2 also shows the extent of the wear on ball and flat sides with and without SPGF after short-duration tests of 600 cycles. As shown in Fig. 2b, the wear scar diameter of steel ball is about 245 µm after sliding against the steel flat. However, the wear scar diameter of ball against SPGF deposited flat is much lower, i.e., about 75 µm (see Fig. 2d). The width of the wear track on the control 440C flat is also very large when compared to that of the flat that was coated with SPGF. From Fig. 2d and e, it is clear that the wear damage was minimal with very little wear mark as well as the wear debris were significantly less in and around the sliding wear scar and track areas of this test pair with SPGF at the sliding interface. The difference in the wear scar diameter on the ball side and the wear track width on the flat side (particularly the wear is always higher on the ball side) is due to the fact that the ball suffers higher Hertzian pressure effects and stays in

contact all the time, while the flat side wear region is in contact periodically. Secondly, variation in the flat sample wear track width from one location to another along the circular wear track may have also contributed to this effect.

We attribute such a dramatic reduction in friction and wear in Fig. 2 to the presence of graphene layers within the sliding wear track, as this was further confirmed by Raman spectroscopy carried out inside the wear track (see Fig. 4).

For better understanding of the beneficial effect of graphene on wear, we used a 3D surface profilometer and obtained line scans profiles and images of the wear tracks after 600 cycle sliding tests. As shown in Fig. 3a, the wear damage on flat remains very insignificant when SPGF is present at sliding interface, but increases substantially for the case where no SPGF was used (see Fig. 3b). After the test, the roughness of the wear track increases markedly indicating that a severe wear situation was in place; while very little wear or scratch marks were present on the flat which was covered by SPGF.

After the completion of the sliding test of 600 cycles (sliding distance of 60 m), when we re-examined the sliding surfaces with Raman microscope, we obtained the Raman spectrum shown in Fig. 4 which proves our hypothesis that graphene was indeed present and had formed a uniform coating within the sliding wear track area. The Raman mapping of the 2D peak (~2700 cm^{-1}, red color corresponds to the highest intensity, blue to the lowest when no peak is present) of the wear track indicates the presence of this peak everywhere in the track, thus further confirming the presence of graphene not only as a smeared tribo-layer (intensity ratio and position of the G and 2D peaks indicate single layer graphene presence), but also as loose flakes within the wear track with its characteristics higher and lower Raman bands.

The defect peak at ~1350 cm^{-1} did not increase as compared to the as deposited condition indicating the graphene layers were almost intact during this shorter-duration test (i.e., 600 sliding cycles), and hence resulted in remarkable improvements in friction and wear. It is interesting to note that despite the dry nitrogen test environment, the friction coefficient of SPGF is very low, which is not the case with highly oriented pyrolitic graphite (HOPG) tested in dry air or inert test conditions [34,35]. This shows unique behavior of SPGF that could be exploited further as a much better solid lubricant than bulk graphite.

3.2. *Effect of SPGF on friction and wear for long duration of cycling*

In order to further explore the durability of these graphene layers, we ran much longer sliding tests of more than 2000 cycles (or 190 m). Fig. 5 compares the frictional behaviors of steel against steel and steel against SPGF deposited steel test pairs.

It is clear that the frictional behavior of steel against steel remains very unsteady as it fluctuates between ≈0.3 and ≈1 during the test. For the steel against graphene coated steel case, the friction coefficient is fairly low (i.e., ≈0.2) for the first 500 cycles, but then it begins to increase and eventually reach values as high as 0.6. It also behaves somewhat similar to steel against steel although with lesser jumps in COF. We attribute such a frictional behavior to the diminishing beneficial effect of graphene as it wears out or loses its effectiveness in the long run. Nevertheless, whatever is left on the sliding wear track still provides substantially lower friction (2 times lower) compared to bare steel against steel case.

For longer duration tests of more than 2000 cycles, the improvements in wear performance due to SPGF were still significant as shown in Fig. 5. Specifically, the wear scar and track formed on the ball and flat sides during steel against steel test were very large as shown in Fig. 5b and c; while the wear scar and track formed on the ball and flat with SPGF on sliding surfaces were much smaller in size despite more than 2000 sliding passes (Fig. 5d and e). Although, the results show increase in the amount of wear for SPGF-covered steel for such longer run (as opposed to shorter, 600 cycles run),

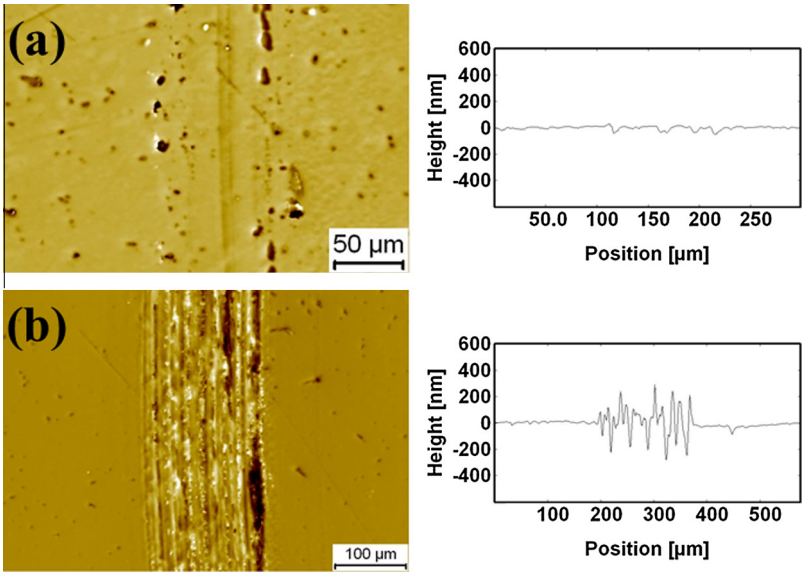

Fig. 3 – Height profile measurements of the wear tracks in dry nitrogen environment for steel against SPGF/steel after 600 cycles (a), and steel against steel after 600 cycles (b).

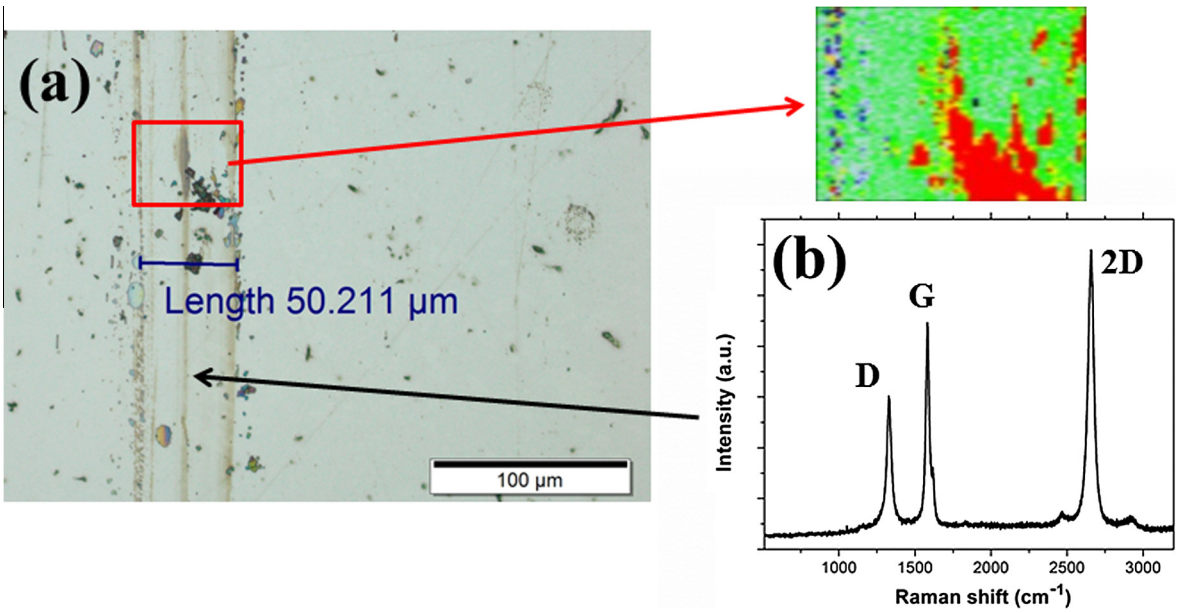

Fig. 4 – (a) Optical image of wear track with protective graphene layers and (b) Raman image (top) and spectrum (below) confirming its presence as a protective coating within the wear track.

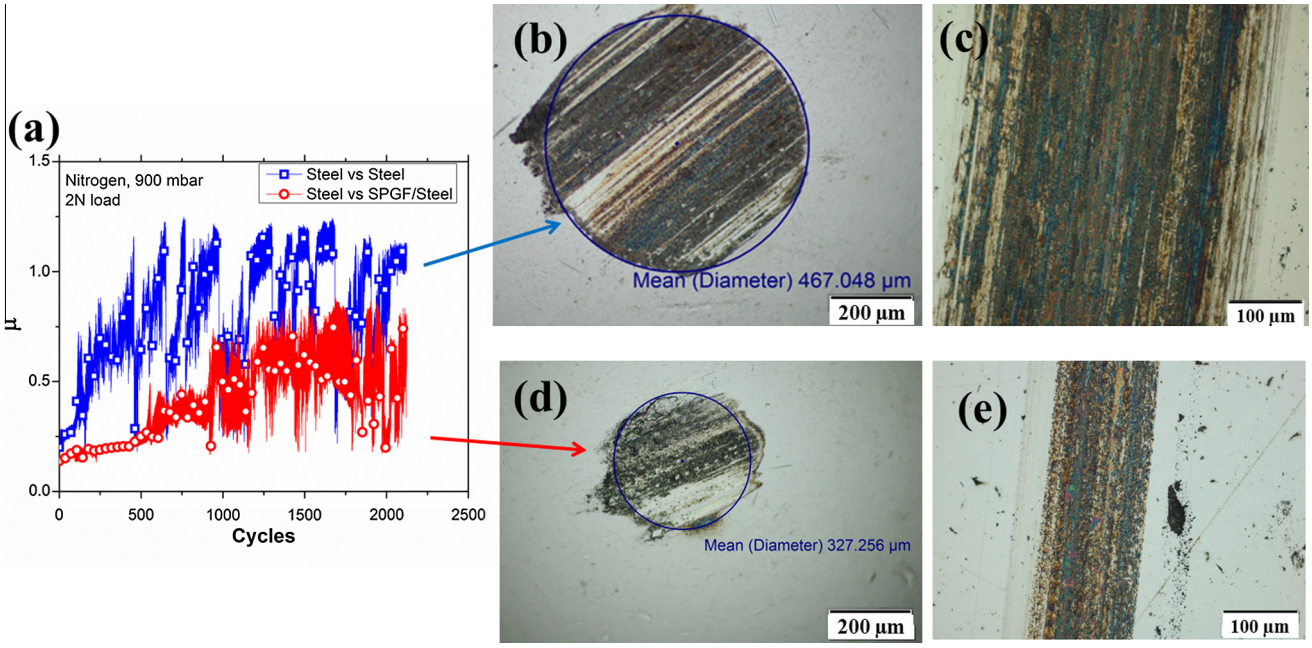

Fig. 5 – Coefficient of friction tests for steel tribo-pairs without SPGF and with SPGF for 2000 cycles (a), and corresponding optical images of the wear scar produced on the ball and plate without SPGF (b and c) and with SPGF (d and e).

it is still significantly lower than that for the bare steel interfaces. This increase in wear is most likely due to the fact that graphene-based protective layer is worn out and the graphene flakes were pushed outside of the wear track, thus after the initially protective period, the sliding contact areas began to experience more and more steel to steel contact resulting in more abrasive wear. Such an increased steel to steel sliding contact is perhaps the main reason for increased and relatively unsteady nature of the friction of this test pair. Despite all these, the friction coefficient and wear scar and track of 440C ball against SPGF-coated 440C are still smaller than those observed on steel against steel test pair suggesting that although much diminished, the beneficial effect of SPGF persists for quite a long time.

Detailed microscopic and Raman studies of the wear scar for SPGF/steel case after the completion of 2000 cycle test (shown in Fig. 6) revealed that the great majority of the graphene layers on the rubbing surfaces was indeed worn out or removed from the wear track. We could only confirm the presence of graphitic flakes near the sliding wear track as op-

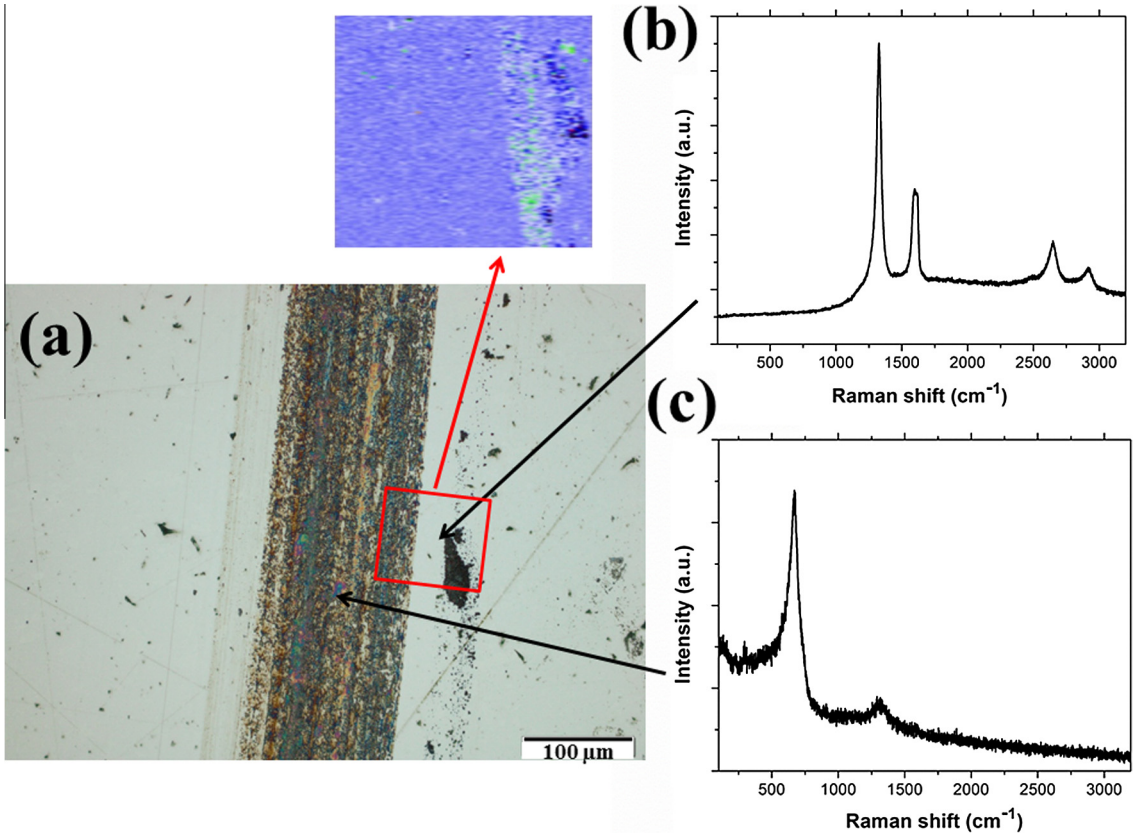

Fig. 6 – SPGF/steel wear track after 2000 cycles (a). The Raman signatures for wear debris outside the wear track (b) and in the wear track (c) are also presented.

posed to within it as shown in Fig. 6. Likewise, the Raman evidence of graphene was found in the wear debris laying outside the wear scars on flat and ball sides as shown in Figs. 6 and 7, respectively and not inside the wear track. 2D peak of graphene looks weak and the disordered peak intensity at ~1350 cm^{-1} becomes much higher ($I_D/I_G \approx 2$ as compared to $I_D/I_G \approx 0.6$ in case of 600 cycles), suggesting significant modifications had occurred to graphene within the contact zone by converting it into the disordered graphitic structure. Raman signature inside the wear track for longer tribo test reveals formation of iron nitrides (at ~673 cm^{-1} and below) [37] and iron oxides (at ~1300 cm^{-1} and 1600 cm^{-1}) [38–40] with no signature of graphene. As it can be expected, the intensity for iron nitrides is higher in nitrogen environment; however, residual oxygen in the system appears to have caused tribo-oxidation of the steel surface as confirmed by some minor iron oxide peaks in Fig. 7 on the ball side.

Moreover, Energy-dispersive X-ray spectroscopy (EDS) analysis performed inside the wear track using Scanning Electron Microscope (SEM) showed that oxygen content in the wear scar increased from 0.4% for the initial 600 cycles run to 9.8% for the prolonged 2000 cycling, thus indicating onset of oxidation of the steel when the graphene protection layer is removed.

The assessment of the wear volume of flat was very difficult as wear was manifested as deep scratches and could not be fit into a reliable wear equation. To estimate the wear volume for the balls after the tribo tests, we used the following equation:

$$V = \left(\frac{\pi h}{6}\right)\left(\frac{3d^2}{4} + h^2\right) \quad (1)$$

where

$$h = r - \sqrt{r^2 - \frac{d^2}{4}} \quad (2)$$

d is wear scar diameter and r is the radius of the ball.

Table 1 presents the results of ball wear volume calculations for shorter- (600 cycles) and longer- (2000 cycles) duration tests based on above equation.

The presented values of the wear show that even small amount of SPGF reduces wear of the steel ball by 2 orders of magnitude during shorter (600 cycle) tests, while the difference is still very significant (i.e., 3 to 4 times lower) for the longer duration tests. These results suggest that graphene could be an excellent solid lubricant for applications involving inert environments.

3.3. *Load dependence*

In above case, we have mostly presented the COF and wear comparison for SPGF effect at 2 N load. It was shown that SPGF can provide excellent protection for the shorter duration (i.e., 600 cycles) tests under a 2 N load. To investigate the

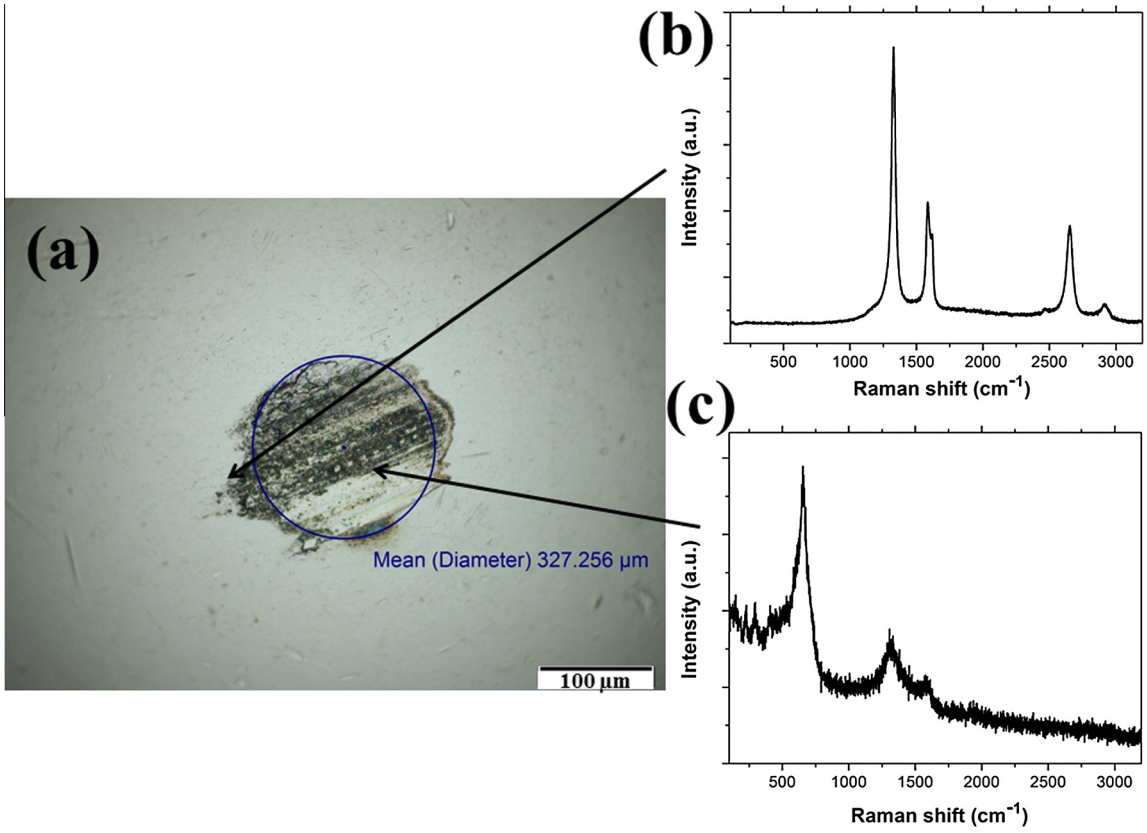

Fig. 7 – Steel ball wear after tribotest with SPGF/steel after 2000 cycles (a). The Raman signatures for wear debris outside the wear track (b) and in the wear track (c) are also presented.

Table 1 – Ball wear volume calculations for 600 and 2000 cycle tests at 2 N load.

Test conditions	Calculated wear volume (600 cycles) (mm^3)	Wear rate (Wear/(load·distance)) (600 cycles) (mm^3/N m)	Calculated wear volume (2000 cycles) (mm^3)	Wear rate (Wear/(load·distance)) (2000 cycles) (mm^3/N m)
Steel/steel	3.7×10^{-5}	3.28×10^{-7}	4.9×10^{-4}	13.05×10^{-7}
With SPGF	3.2×10^{-7}	2.83×10^{-9}	1.2×10^{-4}	4.43×10^{-7}

effect of graphene under lower and higher loads, we performed additional tests under 1, 3 and 5 N loads, respectively keeping rest of the test conditions same. Fig. 8 shows the frictional performance of SPGF under different loads. It is interesting to observe that for 1 N applied load, the COF remains low and steady even after 2000 cycles, while for higher loads of 3 N and 5 N friction increases substantially after about 250 cycles for 3 N load, and 150 cycles for 5 N load.

From these results, it can be concluded that graphene protection is more pronounced at lower loads, while for higher loads, the graphene layer is worn out or quickly removed out of the wear track and hence its beneficial effect is lost. This effect can also be noticed in the wear of 440C balls. As shown in Fig. 9d, the wear volume of ball tested under 5 N load is 4 orders of magnitude higher than that of the ball used under 1 N load; (~10^{-3} mm^3) vs (~10^{-7} mm^3).

Note that in Fig. 8, the highly unsteady and erratic behavior of the coefficient of friction becomes very clear after the initial period where graphene was effective. This proves the fact that after initial run-in time, the protective graphene layer is perhaps removed out of the wear track and the sliding surfaces were experiencing more and more metal-to-metal contact and thus higher and higher levels of adhesion and hence friction. The longest durability or lifetime of the SPGF layer was achieved under the lowest load (i.e., 1 N). It should be emphasized, that all of these tests were performed on steel surfaces at a very low concentration (i.e., 1 mg/l) of graphene flakes which resulted in partial graphene coverage (see Fig. 1) or graphene islands on sliding surfaces. Thus, increasing the concentration or continuous replenishment of the graphene flakes on sliding contact interface during sliding tests could potentially lower friction and wear further and for much longer periods of time. Constant feeding of graphene solution has been shown before to be effective for wear protection in humid air environment [33].

In this study we show, that the graphene protective layer can stay for more than 2000 cycles, thus reducing friction and wear and inhibiting the steel corrosion. Moreover, we

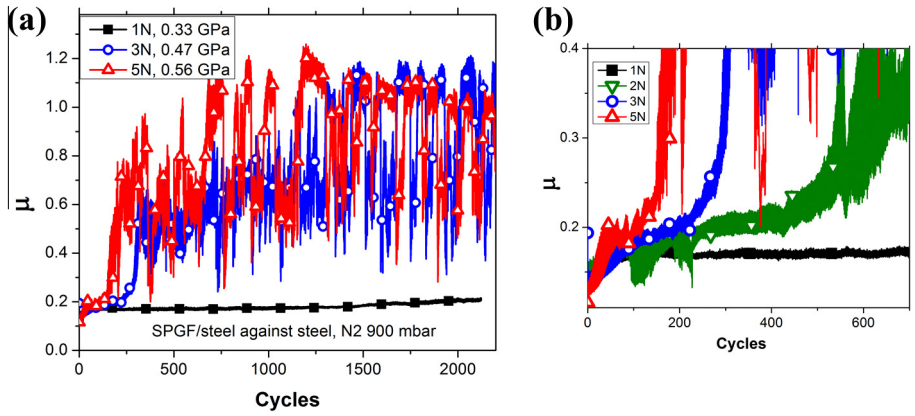

Fig. 8 – Coefficient of friction for steel with SPGF under different loads (a) for 2000 cycles; (b) represents magnified view for initial cycling period. The average Hertz contact pressure is presented for every applied load.

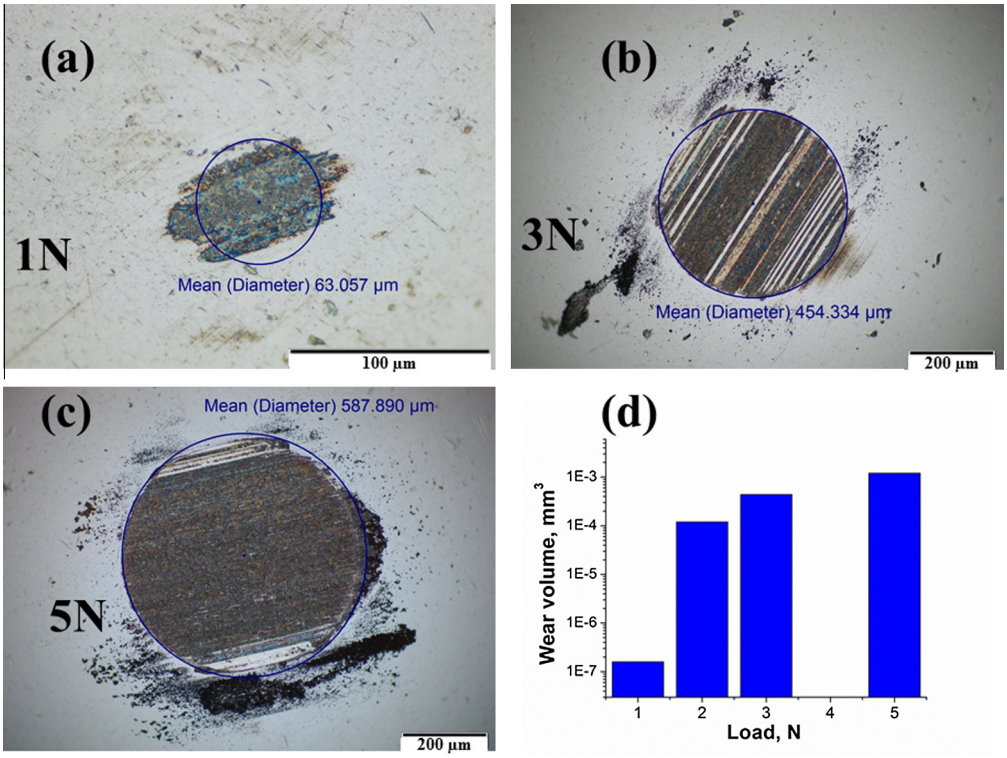

Fig. 9 – Ball wear after 2000 cycles for SPGF/steel against steel under different loads: 1 N load (a), 3 N load (b), and 5 N load (c). The calculated ball wear volume for different loads is presented in (d).

show that graphene application as well as re-application does not require any additional processing steps other than just sprinkling a small amount of ethanol solution on the surface of interest making this process simple, cost effective, and environmental friendly.

4. Conclusions

A series of experiments were conducted to compare the effect of graphene on friction and wear behavior of 440C steel in dry nitrogen environment.

The results indicate that small amounts of graphene on the sliding surface are able to afford reasonably low friction coefficients (i.e., 0.15–0.3) compared to very high and unsteady friction of steel without graphene. Moreover, the wear volume of graphene lubricated test pair is 2 orders of magnitude smaller than that of bare 440C for 600 cycle tests. Such marked reductions in friction and the wear are attributed to the low shear and highly protective nature of the graphene which also prevented oxidation and nitride formation when present at sliding contact interfaces. The tribo tests under different load regimes show a clear dependence of the lifetime of the graphene layer on the contact severity. Under very heavy loads, like 5 N, graphene was removed from the sliding surface instantly which resulted in high friction and wear from the very beginning of sliding tests; while under the lightest

load of 1 N, graphene layer could last for the entire duration of 2000 cycle test and afford very low friction and wear (4 orders of magnitude lower than for 5N load). Overall, our experimental results demonstrate that graphene holds great promise as an effective solid lubricant for moderate loads and can be easily deposited on tribological surfaces by the use of SPG containing graphene flakes.

Acknowledgments

Use of the Center for Nanoscale Materials was supported by the US Department of Energy, Office of Science, Office of Basic Energy Sciences, under Contract No. DE-AC02-06CH11357.

REFERENCES

[1] Donnet C, Erdemir A. Solid lubricant coatings: recent developments and future trends. Tribol Lett 2004;17:389–97.
[2] Maboudian R, Ashurst WR, Carraro C. Tribological challenges in micromechanical systems. Tribol Lett 2002;12:95–100.
[3] Ludema KC. Friction, wear, lubrication: a textbook in tribology. Florida: CRC Press, Inc.; 1993. p. 69–155.
[4] Lancaster JK. A review of the influence of environmental humidity and water on friction, lubrication and wear. Tribol Int 1990;23:371–89.
[5] Spikes H. The history and mechanisms of ZDDP. Tribol Lett 2004;17:469–89.
[6] Liu WM, Ye CF, Gong QY, Wang H, Wang P. Tribological performance of room-temperature ionic liquids as lubricant. Tribol Lett 2002;13:81–5.
[7] Pit R, Marchon B, Meeks S, Velidandla V. Formation of lubricant "moguls" at the head/disk interface. Tribol Lett 2001;10:133–42.
[8] Khorramian BA, Iyer GR, Kodali S, Natarajan P, Tupil R. Review of antiwear additives for crankcase oils. Wear 1993;169:87–95.
[9] Sofo JO, Chaudhari AS, Barber GD. Graphane: a two-dimensional hydrocarbon. Phys Rev B 2007;75:153401.
[10] Geim AK, Novoselov KS. The rise of graphene. Nat Mater 2007;6:183–91.
[11] Lee H, Lee N, Seo Y, Eom J, Lee SW. Comparison of frictional forces on graphene and graphite. Nanotechnology 2009;20:325701.
[12] Lee C, Li Q, Kalb W, Liu X-Z, Berger H, Carpick RW, et al. Frictional characteristics of atomically thin sheets. Science 2010;328:76–80.
[13] Filleter T, McChesney JL, Bostwick A, Rotenberg E, Emtsev KV, Seyller T, et al. Friction and dissipation in epitaxial graphene films. Phys Rev Lett 2009;102:086102.
[14] Bollmann W, Spreadborough J. Action of graphite as a lubricant. Nature 1960;186:29–30.
[15] Schwarz UD, Zworner O, Koster P, Wiesendanger R. Quantitative analysis of the frictional properties of solid materials at low loads. Phys Rev B 1997;56:6987–96.
[16] Lee CG, Wei XD, Kysar JW, Hone J. Measurement of the elastic properties and intrinsic strength of monolayer graphene. Science 2008;321:385–8.
[17] Lee C, Wei X, Li Q, Carpick R, Kysar JW, Hone J. Elastic and frictional properties of graphene. Phys Status Solidi B 2009;246:2562–7.
[18] Gómez-Navarro C, Burghard M, Kern K. Elastic properties of chemically derived single graphene sheets. Nano Lett 2008;8:2045–9.
[19] Gao YW, Hao P. Mechanical properties of monolayer graphene under tensile and compressive loading. Physica E 2009;41:1561–6.
[20] Marchetto D, Held C, Hausen F, Wählisch F, Dienwiebel M, Bennewitz R. Friction and wear on single-layer epitaxial graphene in multi-asperity contacts. Tribol Lett 2012;48:77–82.
[21] Choudhary S, Mungse HP, Khatri OP. Dispersion of alkylated graphene in organic solvents and its potential for lubrication applications. J Mater Chem 2012;22:21032–9.
[22] Huanga HD, Tua JP, Ganb LP, Li CZ. An investigation on tribological properties of graphite nanosheets as oil additive. Wear 2006;261:140–4.
[23] Lin J, Wang L, Chen G. Modification of graphene platelets and their tribological properties as a lubricant additive. Tribol Lett 2011;41:209–15.
[24] Gupta BK, Bhushan B. Fullerene particles as an additive to liquid lubricants and greases for low friction and wear. Lubricat Eng 1994;50:524–8.
[25] Lin J, Wang L, Chen G. Modification of graphene platelets and their tribological properties as a lubricant additive. Tribol Lett 2011;41:209–15.
[26] Kandanur SS, Rafiee MA, Yavari F, Schrameyer M, Yu ZZ, Blanchet TA, et al. Suppression of wear in graphene polymer composites. Carbon 2012;50:3178–83.
[27] Stankovich S, Dikin DA, Dommett GHB, Kohlhaas KM, Zimney EJ, Stach EA, et al. Graphene-based composite materials. Nature 2006;442:282–6.
[28] Erdemir A. Solid lubricants and self-lubricating films. In: Bhushan B, editor. Modern tribology handbook. Boca Raton, FL: CRC Press; 2001. p. 787–818.
[29] Spreadborough J. The frictional behaviour of graphite. Wear 1962;5:18–30.
[30] Wahl KJ, Seitzman LE, Bolster RN, Singer IL. Low friction, high endurance ion-beam deposited Pb–Mo–S coatings. Surf Coat Technol 1995;73:152–9.
[31] Hilton MR, Bauer R, Didziulis SV, Dugger MT, Keen JM, Scholhamer J. Structural and tribological studies of mos2 solid lubricant films having tailored metal-multilayer nanostructures. Surf Coat Technol 1992;53:13–23.
[32] Donnet C, Martin JM, LeMogne T. Super-low friction of MoS_2 coatings in various environments. Tribol Int 1996;29:123–8.
[33] Berman D, Erdemir A, Sumant AV. Graphene enabled reduced wear and friction in sliding steel surfaces. Carbon 2013;54:454–9.
[34] Bryant PJ, Gutshall PL, Taylor LH. A study of mechanisms of graphite friction and wear. Wear 1964;7:118–26.
[35] Buckley DH, Brainard WA. Friction and wear of metals in contact with pyrolytic graphite. Carbon 1975;13:501–8.
[36] Ferrari AC. Raman spectroscopy of graphene and graphite: disorder, electron–phonon coupling, doping and nonadiabatic effects. Solid State Commun 2007;143:47–57.
[37] Nakamoto K. Resonance Raman spectra and biological significance of high-valent iron (IV, V) porphyrins. Coord Chem Rev 2002;226:153–65.
[38] Hanesch M. Raman spectroscopy of iron oxides and (oxy)hydroxides at low laser power and possible applications in environmental magnetic studies. Geophys J Int 2009;177:941–8.
[39] Maslar JE, Hurst WS, Bowers WJ, Hendricks JH. In situ Raman spectroscopic investigation of stainless steel hydrothermal corrosion. Corrosion 2002;58:739–47.
[40] Thanos ICG. Electrochemical reduction of thermally prepared oxides of iron and iron–chromium alloys studied by in situ Raman spectroscopy. Electrochim Acta 1986;31:1585–95.